Published in final edited form as:
J Immunol. 2013 September 15; 191(6): 3169–3178. doi:10.4049/jimmunol.1301106.

B cell intrinsic and extrinsic regulation of antibody responses by PARP14, an intracellular ADP-ribosyltransferase

Sung Hoon Cho[*], **Ariel Raybuck**[*], **Mei Wei**[*], **John Erickson**[*,†], **Ki Taek Nam**[‡], **Reagan G. Cox**[*,†], **Alyssa Trochtenberg**[*], **James W. Thomas**[*,§], **John Williams**[*,†], and **Mark Boothby**[*,§,#]

[*]Department of Pathology, Microbiology & Immunology, Vanderbilt University School of Medicine, Nashville, TN 37232

[†]Department of Pediatrics, Vanderbilt University School of Medicine, Nashville, TN 37232

[§]Department of Medicine, Vanderbilt University School of Medicine, Nashville, TN 37232

[‡]Severance Biomedical Science Institute, Yonsei University College of Medicine, Seoul 120-752, Korea

Abstract

The capacity to achieve sufficient concentrations of Ag-specific Ab of the appropriate isotypes is a critical component of immunity that requires efficient differentiation and interactions of Ag-specific B and T helper (Th) cells along with dendritic cells. Numerous bacterial toxins catalyze mono-(ADP-ribosyl)ation of mammalian proteins to impact cell physiology and adaptive immunity. However, little is known about biological functions of intracellular mammalian mono-(ADP-ribosyl)transferases (mART), such as any ability to regulate Ab responses. Poly-(ADP-Ribose) Polymerase 14 (PARP14), an intracellular protein highly expressed in lymphoid cells, binds to STAT6 and encodes a catalytic domain with mART activity. Here we show that recall IgA as well as the STAT6-dependent IgE Ab responses are impaired in PARP14-deficient mice. Whereas PARP14 regulation of IgE involved a B cell intrinsic process, the predominant impact on IgA was B cell-extrinsic. Of note, PARP14 deficiency reduced the levels of Th17 cells and $CD103^+$ DCs which are implicated in IgA regulation. PARP14 enhanced the expression of RORα, Runx1 and Smad3 after T cell activation, and, importantly, its catalytic activity of PARP14 promoted Th17 differentiation. Collectively, the findings show that PARP14 influences the class distribution, affinity repertoire, and recall capacity of antibody responses in mice, and provide direct evidence of requirement for protein mono-ADP-ribosylation in T helper differentiation.

INTRODUCTION

Adaptive immunity depends on the level and effector functions of specific helper T cell subsets and the antibody classes and affinities generated as a consequence of antigenic challenge. Moreover, these features are determinants of vaccine efficacy as well as immune-mediated diseases and their pathology (1, 2). Circulating antibodies are produced and secreted by plasma cells after B cell activation, proliferation, and differentiation (2, 3). In addition to a crucial impact of Ab concentrations, their functions are determined by affinity and the Ig heavy chain class or isotype in addition to the exact epitope recognized (4). Thus, the Fc region for IgE initiates classical complement fixation very inefficiently compared to several IgG isotypes. Notwithstanding differences between mice and humans, IgE is a key mediator of allergic diseases and protection against extracellular parasites, functions

[#]Correspondence: Mark Boothby, Dept of Pathology, Microbiology & Immunology, Vanderbilt University School of Medicine, Nashville, TN 37232-2363, Tel: 615-343-1699, FAX: 615-343-7392, Mark Boothby at mark.boothby@vanderbilt.edu.

mediated by specific binding to FcεR1, a class-specific high-affinity receptor present on mast cells and basophils (5, 6). IgA also fails to initiate classical complement fixation (7) but is crucial for managing host-microbe interactions at mucosal surfaces such as the airways and gut (8). Moreover, Fc receptors for these Ig classes differ in their downstream effects and species-specific expression (9). Thus, molecular mechanisms that adjust the levels of different classes of Ig and the balance among them are important aspects of immunity.

In the primary Ab response, activation of naïve IgM/IgD-expressing B cells leads to a variety of potential fates, the probability of each of which is dictated by the locale or trafficking of the B lymphoblast and interactions with helper $CD4^+$ T cells and the cytokines they produce (10, 11). B cells that receive cognate T cell help can enter the germinal center reaction and, if they survive affinity selection, are better able to differentiate into memory B cells or progress to become long-lived antibody-secreting plasma cells (10–12). When the cytokine IL-4 predominates, B cells switch their Ag-specific V_H segment to the IgH Cε region, either directly from Cμ or as a secondary gene rearrangement from the IgH Cγ1 segment (13, 14). The ontogeny of cellular identity and gene regulation within the helper T cell population are fluid, but $CD4^+$ T cells are the predominant source of IL-4 to promote class switching to IgE under physiological conditions (13, 15). To provide this cytokine, Ag-activated T cells adopt gene expression programs of T helper 2 (Th2), IL-4-producing T follicular helper, or Th2-derived T_{FH} phenotypes (T_{FH}, or $T_{FH}2$) (16, 17). A variety of signaling combinations can induce IL-4-producing Th2 or $T_{FH}2$ cells, but these processes are potentiated or amplified by IL-4 and its induction of the transcription factor STAT6 (18, 19). In addition to this B cell-extrinsic impact of STAT6, IL-4 and STAT6 are required for B cell-intrinsic aspects of class switching to IgE and, to a lesser extent, to IgG1 (20–22).

The regulators of class switching to IgA are more complex, as a number of factors have been elucidated (23). The most important soluble regulators of IgA production include TGF-β, retinoic acid (RA), the type 2 cytokine IL-5 (23, 24). Cell trafficking to gut and other mucosal sites are major factors, so that the intestinal tract and its associated lymphoid tissues are major sites for IgA generation (25), but prominent drivers of IgA production (i.e., TGF-β and RA) are not T helper subset-specific products (23, 26). However, one subset of dendritic cells (DC), the $CD103^+$ DC population, is the major source of RA implicated in generation of IgA^+ B cells, whereas the TGF-β-rich environment promotes an environment highly enriched for IL-17 and -22-producing Th17 cells (27, 28). Strikingly, recent work indicates that Th17 cells drive IgA production (29). Nonetheless, IL-4 has the capacity to enhance the generation of IgA-positive B cells when combined with primary regulators (30, 31). More broadly, the discovery of a Th2 phenotype identified a capacity of this T cell subset to promote Ab responses (32, 33), and recent work involving T_{FH} cells showed dramatic decreases in antibody-secreting cells located in the marrow in models of Ag-specific immunity when IL-4 or its receptor was absent (17).

Recall antibody responses in turn draw on the formation of Ag-specific memory B cells from either IgM^+ or isotype-switched B lymphoblasts after primary immune exposure (2). In parallel, the pool of circulating Ab can be sustained by an alternative fate in which plasmablasts become long-lived plasma cells that constitutively secrete Ab for extended periods of time. Memory subsets arise most efficiently after T cell help and an effective germinal center reaction (2, 3) involving B cells that survive BCR selection for survival but do not become plasma cells (10). Long-lived plasma cells are vital for steady-state production of Ag-specific Ab that may neutralize a pathogen after re-exposure, but these cells and the circulating Ab they produce decline over time, albeit at different rates for Ab isotypes and different forms of immunogen (10). Thus, the memory B cell pool can provides vital back-up mechanism whereby recall Ag stimulates renewed B cell activation, differentiation into plasma cells, and increased circulating Ab. Although this recall

stimulation commonly requires renewed T cell help, the molecules and mechanisms that influence the strength of recall Ab responses need elucidation.

As noted above, IL-4 and STAT6 regulate both B cell-extrinsic regulation of Ab responses via T helper function and B cell-intrinsic processes. STAT6 heterodimers act as DNA binding proteins that recruit transcriptional cofactors to a unique palindromic element (18), but little is known about specific cofactors in antibody responses. Poly-(ADP-ribose) Polymerase (PARP)14, a novel STAT6-interacting protein with transcriptional cofactor function, is in a super-family of proteins with domains similar to those of bacterial toxins that transfer ADP-ribose from NAD^+ onto target proteins (34). Initial analyses revealed that PARP14 increased mRNA levels for a subset of STAT6-regulated genes in B cells and enhanced survival signaling initiated by IL-4 treatment of B (but not T) lymphocytes in vitro (35). Subsequent work showed that PARP14 facilitates lymphomagenesis driven by persistent over-expression of the oncogene *c-Myc*, is vital for a Myc-imposed block at the pre-B stage of B lymphoid development, and helps to transduce an IL-4 signal that promotes metabolic fitness and survival of mature B cells (36). Furthermore, recent findings indicate that c-Myc is a major regulator of germinal center B cells and show an impact of PARP14 on survival of plasmacytoma cells (37–39). However, to what extent the defects observed in the absence of PARP14 impair antibody responses after infection or affect recall responses is not clear. In the present study, we have analyzed the contributions of PARP14 to primary and recall antibody responses in disease models of infection with a common respiratory pathogen and of allergic lung inflammation. Surprisingly, Ag-specific IgA and IgE production were both impaired while IgG1 was not, but analyses of the cellular basis for IgA and IgE defects revealed both B cell-dependent and -independent mechanisms along with a defect in potency of T helper effectors. Further, the results provide insight into an unexpected parallel between functions of microbial ADP-ribosylating toxins and an intracellular mammalian ADP-ribosyltransferase, and have important implications in relation to potential new avenues for pharmacological intervention in immunity.

MATERIALS & METHODS

Mice and B cell transfer model

All mice [C57BL/6 (JAX; Bar Harbor, ME), B6-*Rag2* −/−, B6-*Parp14* −/− mice, B6-OT-II TCR transgenic, and B6/129-intercrossed *Stat6* −/−] were housed in ventilated micro-isolators under Specified Pathogen-Free conditions in a Vanderbilt University mouse facility and used at 6–8 wk of age following approved protocols. For adoptive transfer experiments to measure Ab responses, T cells were depleted using biotinylated anti-Thy1.2 Ab followed by streptavidin-conjugated microbeads (iMag™; BD Biosciences, San Jose CA). Pooled WT $CD4^+$ T cells and OT-II $CD4^+$ T cells (4 and 1×10^6cells per recipient, respectively) purified by positive selection with L3T4 anti-CD4 microbeads (40) were mixed with pools of WT or *Parp14* −/− B cells (5×10^6cells per recipient) and injected intravenously (i.v.) into *Rag2* −/− recipients.

Reagents

Cytokines and mAb (purified, biotinylated, or fluorophore-conjugated) were from BD-Pharmingen unless otherwise indicated. NP and NIP-conjugated serum albumins (for capture ELISA) and carrier proteins (KLH; ovalbumin) were obtained from Biosearch (Novato CA). All-trans retinoic acid, DNase I, chicken ovalbumin (41), LPS (42) and collagenase (C. histolyticum Type VIII) were from Sigma-Aldrich Chemicals (St. Louis MO). IL-4 and IL-5 were obtained from Leinco Technology (St. Louis, MI), and TGFβ and BAFF were from R&D Systems (Minneapolis, MN).

Infections, immunizations, and measurements of Ab responses

After collection of pre-immune sera, mice were immunized with NP_{25}-KLH (100 μg intraperitoneally) in alum (Imject, Thermo Scientific, Rockford IL) as described (41). Primary immune sera were collected after 2 wk, followed by pre-boost serum collection, an identical recall immunization 5 wk thereafter, and harvest 1 wk later for analyses. To immunize and rechallenge in the context of primary and recall allergic lung inflammation, mice were sensitized with ovalbumin (OVA; 20 μg per mouse) in alum (41) on day 0 and 7, followed after 14 d by intranasal OVA (50 μL of OVA, 10% w/v in buffered saline) instillations on each of 4 consecutive days. For recall IgE responses and allergic lung inflammation, mice (primary Ag inhalations 7 wk previously) were harvested the day after ending intranasal OVA re-challenges (exactly as for primary responses) on each of 4 consecutive days. Broncho-alveolar lavage (BAL) fluid sampling and counting of airway cell populations were conducted as described (41). Cytokine levels in BAL fluid were measured by Milliplex mouse cytokine/chemokine Luminex kit (32-plex) (EMD-Millipore, Billerica, MA) according to manufacturer's instructions. Lung inflammation and airway mucus were determined based on hematoxylin & eosin and Periodic acid-Schiff (PAS) stained, paraffin-embedded lung sections. Airway mucus was measured by a pathologist blind to sample identity, using a semiquantitative grading system based on the fraction of PAS^+ airway epithelial cells [*grade 0*, no PAS staining; *grade 1*, <20%; *grade 1.5*, 21–40%; *grade 2*, 41–60%; *grade 2.5*, 61–80%; *grade 3*, >81%]. For infectious challenges, mice were infected with human metapneumovirus (hMPV) (1.5×10^6 PFU by intranasal instillation under anesthesia) with a clinical isolate strain as described (43), followed by collection of primary immune sera after 3 wk. At 14 wk post-infection, mice were re-challenged in identical manner, and harvested 1 wk later for analyses. After first establishing dilutions at which absorbance values would be in the linear range of the assay, isotype-specific relative levels of Ag-specific Ab were quantitated by ELISA using plate-bound Ag ([NP-BSA or PSA, OVA, or purified, recombinant hMPV F protein (44)] followed by the series of isotype-specific second Ab of the SBA Clonotyping System (Southern Biotech, Birmingham AL), as described (41). Data for Ag-specific Ab are shown after subtraction of low OD values from pre-immune controls analyzed together with the immune sera and were separately determined to match values yielded by titration. Ab-secreting cells (ASC) were analyzed by ELISpot as previously described (41) and quantitated using an ImmunoSpot Analyzer (Cellular Technology, Shaker Heights OH).

In vitro B cell cultures for class-switched Ab production

Splenic B cells were purified (90–95%) using biotinylated anti-CD19 mAb followed by streptavidin-conjugated microbeads as above. For IgA, B cells (10^6 cells in 1 ml) were activated with LPS (1 μg/ml) and cultured with BAFF (10 ng/ml), TGF-β (5 ng/ml), IL-4 (10 ng/ml), IL-5 (10 ng/ml), and all-trans retinoic acid (RA) (10 nM) in 10% FBS-supplemented medium exactly as described (24). Surface IgA was analyzed by flow cytometry with cells harvested at 5 d, and culture supernatants were then harvested after 7 d to measure IgA in the culture supernatants. For IgE, B cells (10^6cells in 2 ml) were activated with anti-CD40 (1 μg/ml; clone 3/23) (45), cultured with BAFF, IL-4, and IL-5 as for IgA analyses, followed by determination of intracellular IgE by flow cytometry and ELISA to measure secreted IgE as described previously (46).

$CD103^+$ DC analysis

Preparations of mononuclear cells of the mesenteric lymph nodes (MLN), Peyer's Patches (PP), intestinal lamina propria (LP), and intra-epithelial compartments (IEC) were prepared from WT and *Parp14* −/− mice as described (47). In brief, small intestines were flushed with FBS 10% in CMF solution (Hank's Balanced Salt Solution (HBSS) supplemented with HEPES and $NaHCO_3$ pH 7.2) followed by removal of Peyer's Patches. Intestinal segments

were then incised lengthwise, minced into 10% FBS in CMF solution with 0.1 mM EDTA after mechanical removal of their mucus layers, shaken (45 min; 37°C), and passed through a 70 μm aperture strainer. IEC were collected from these eluates at the interface of 40–70% Percoll step gradients. The remaining tissue was then digested in 5% FBS in HBSS containing collagenase (1.5 mg/ml) and DNase1 (50 units/ml), and LP cells were collected as the cells at the interface after the resulting cell suspensions were fractionated on 40–70% Percoll step gradients. After counting, populations were analyzed by flow cytometry or RNA was extracted for analysis.

Mutagenesis and ART activity assay

ADP-ribosyltransferase dead mutants of PARP14 and PARP14(M-C) were generated in pcDNA3 and the retrovector MiT by introductions of point mutations into the C-terminal catalytic domain using *Pfu* polymerase; the mutations and non-mutated complete sequence of each construct was verified by DNA sequencing. Lysates of FNX cells transfected with WT or triple-mutated constructs of pcDNA3-FLAG-PARP14 or pcDNA3-FLAG-PARP14-MC were used for immune precipitations with monoclonal anti-FLAG (M2) (Sigma-Aldrich). The resulting immune complexes, collected using protein G beads (Santa Cruz Biotechnology, Santa Cruz, CA), were rinsed and divided equally. Eluted proteins from one portion were analyzed by immunoblotting visualized and quantitated using an Odyssey imaging system (Li-Cor, Lincoln NE) as described (40), while ADP-ribosyl transferase activity in the other fraction was assayed as described (35), with resolution on SDS-PAGE followed by autoradiography, and quantified by Phosphor-Imaging. The specific activities of each construct were estimated by normalization of the ^{32}P-automodified protein signal to the steady-state expression level quantified by immunoblotting.

T helper cell differentiation and retrovector transduction

Naïve CD4$^+$ T cells purified (95%) using anti-CD4 magnetic microbeads (Miltyeni, Auburn CA) and activated with plate-bound anti-CD3 plus soluble anti-CD28 (2.5 μg/ml each) were cultured in T helper subset differentiating conditions [Th1, anti-IL-4 (5 μg/ml) and IL-12 (10 ng/ml); Th2, anti-IL-12 (3 μg/ml), anti-IFN-γ (3 μg/ml), and IL-4 (10 ng/ml); Th17, TGF-β (5 ng/ml), IL-6 (10 ng/ml), TNFα (10 ng/ml), IL1-β (5 ng/ml), IL-23 (10 ng/ml), anti-IL-4 (5 μg/ml), and anti-IFN-γ (3 μg/ml)] as described (40). MiT retrovector constructs were transfected into ΦNX ecotropic packaging cells, whose supernatant media were then used for 'spinfection' of activated CD4$^+$ T cells as described (40). For retroviral transduction to test Th17 differentiation capacity, activated T cells were initially cultured in Th_{Null} conditions [anti-IL-4 (5 μg/ml), anti-IL-12 (3 μg/ml), anti-IFN-γ (3 μg/ml)] to block differentiation. For quantitation of mRNA levels, RNA were isolated after 5 d culture, while measurements of differentiation and cytokine production were performed after secondary stimulation, using intracellular cytokine staining or culture supernatants of T cells, respectively. Cells were re-stimulated with plate-bound anti-CD3 and soluble anti-CD28 (0.5 μg/ml each), and either stained for intracellular IFN-γ, IL-4 and IL-17 along with surface CD4, as described (40), or cultured without monensin. Cytokine concentrations in culture supernatants were measured using a multiplex Th1/2/17 Cytokine Bead Array (BD Pharmingen).

Measurements of RNA

RNA was isolated using Trizol reagent (Invitrogen). After cDNA synthesis by reverse transcription, expression of genes was analyzed in duplicate samples using SYBR green PCR master-mix (Qiagen, Valencia CA) by quantitative real-time RT-PCR (qRT^2-Supplemental Table 1. Data are presented as values normalized to WT control and averaged over PCR) normalized to levels of HPRT as internal control. Primer pairs are detailed in three independent biological replicates.

Statistical analyses

The primary analyses comparing values for WT and *Parp14 −/−* samples were conducted as two-tailed Student's *t* test with post-test validation of its suitability. The analyses consisted of separate pairwise determinations, but 2-way ANOVA were also conducted across aggregate IgA and IgE responses to deal with potential concern about multiple testing. Data are expressed as mean (± SEM), and results were considered statistically significant when the p value for the null hypothesis a comparison was <0.05.

RESULTS

Role for PARP14 in Ag-specific IgA responses

Previous work identified a STAT6-interacting transcriptional co-activator, PARP14, showed it to be an intracellular ADP-ribosyltransferase. Surprisingly, later investigation uncovered an apparently selective defect in survival and glycolytic fitness of B cells from *Parp14 −/−* mice and a need for PARP14 in facilitating certain actions of c-Myc (36), which is vital for sustaining fully robust germinal center reactions (38, 39). Accordingly, we hypothesized that PARP14 would impact antibody responses, particularly those of higher affinities and the classes whose Ig heavy chain constant regions are most distant from IgH Cμ. Because of the utility of hapten-conjugate systems in dissection of Ab response mechanisms, we first tested primary and recall Ab responses after immunizations of WT and *Parp14 −/−* mice with NP-KLH (48). The primary and recall Ab levels for total Ig, IgM, and IgG1 (which dominate the total Ig pool) did not consistently differ between *Parp14 −/−* mice and controls (Supplemental Fig. S1A, B). However, recall responses of IgA (and, to a more modest extent, those of IgG2a and IgG2b) were substantially lower in the absence of PARP14 (Fig. 1; Supplemental Fig. S1C, D). In addition to a decrease in anti-NP IgA in the early primary response (Fig. 1B), the relative impairment of mice lacking PARP14 was worse after recall immunization at 7 wk than at the earlier time (Fig. 1B, C; Supplemental Fig. S1G). The germinal center reaction promotes a heteroclitic response that generates NIP-reactive Ab after NP immunization (48), and affinity maturation of the Ab repertoire (12). Levels of NIP-reactive IgA and high affinity (NP_2-binding) IgA in recall immune sera were also lower in *Parp14 −/−* mice compared to controls (Fig. 1C). Moreover, the serum levels of total IgA, independent of Ag, were lower in the PARP14-deficient mice than WT controls (Supplemental Fig. S1E). To determine if PARP14 influences the generation of IgA reactive against a pathogen that infects mice by a mucosal route, we used a human metapneumovirus (hMPV) infection model (Fig. 1D). As with immunization (Ag in alum), *Parp14 −/−* mice generated lower levels of virus-specific serum IgA in the early primary response (at peak infection) and the gap between wild type and PARP14-deficient mice was widened for IgA-anti-MPV in memory responses elicited by virus rechallenge [Fig. 1E; mean increases of recall over primary IgA levels in *Parp14 −/−* sera (0.114) were one-third those of WT controls (0.377), p=0.03]. A similar pattern, matching that with NP-KLH, was also observed for IgG2a (Supplemental Fig. S1F). Moreover, fewer anti-MPV IgA-secreting cells were detected in infected lungs of the PARP14-null animals (Fig. 1F). Together, these results demonstrate that PARP14 plays a crucial role in promoting IgA production.

B cell extrinsic role of PARP14 in IgA regulation

Recent findings suggest that the Th17 subset and the prevalence of $CD103^+$ DCs are major determinants of the magnitude of an IgA response (26, 28, 29). To dissect the mechanism of how PARP14 regulates IgA generation, we first investigated whether the mechanism was predominantly intrinsic or extrinsic to B lineage cells. WT $CD4^+$ T cells were mixed with WT or *Parp14 −/−* B cells and transferred into *Rag2 −/−* mice that were then immunized to score primary and recall Ab responses (Fig. 2A). Serum anti-NP IgA levels and numbers of NP-specific IgA-secreting cells were comparable in recipient mice that received *Parp14 −/−*

B cell transfers as compared to controls (Fig. 2B). These results provide evidence that a B cell-extrinsic defect led to impaired IgA production in *Parp14* −/− mice. TGFβ and retinoic acid (RA) substantially induce IgA in vitro (49), which is also promoted by IL-5 (49) and IL-4 (49). Preliminary tests indicated that a combination of all these inducers (TGFβ, RA, IL-4, and IL-5) yielded maximum fractions of surface IgA^+ B cells and levels of secreted IgA in the medium (data not shown). The frequencies of membrane IgA^+ B cells (Fig. 2C) and amounts of secreted IgA (Fig. 2D) were equivalent when purified B cells from *Parp14* −/− and WT controls were then activated and cultured under these (Fig. 2C, D) and other (data not shown) conditions. Together, these results suggested that the intrinsic capacities to switch to the distal IgH constant region gene segment Cα and to yield IgA production are intact in *Parp14* −/− B lineage cells, thereby implicating a B cell extrinsic defect.

Impact of PARP14 on B cell-extrinsic regulators of IgA

T helper (Th) cells directly and indirectly regulate most steps of the Ag-specific response and B lineage memory. Th17 cells are particularly prevalent at intestinal mucosal sites, and, along with $CD103^+$ DCs, strongly promote the IgA fate for B lineage cells (29). Moreover, IL-17 deficient mice have impaired IgA physiology, suggesting a role for Th17 cells in IgA generation. When we tested T helper development in vitro, PARP14-deficient $CD4^+$ T cells were altered in their Th17 potential. Thus, WT $CD4^+$ T cells yielded high frequencies of IL-17 positive cells, whereas this was reduced by half for *Parp14* −/− $CD4^+$ T cells (Fig. 3A; Table I). Consistent with these results, IL-17 secretion by *Parp14* −/− Th17 cells was also decreased (Fig. 3B). Since PARP14 functions as a co-factor for a subset of STAT6-dependent functions of IL-4, we tested if this unexpected effect of PARP14 on Th17 cell differentiation impacted other T helper subsets. This analysis indicated that Th2 production of IL-4 by *Parp14* −/− $CD4^+$ T cells was impaired (Fig. 3B), along with a trend toward diminished IFN-γ secretion and lower frequencies of Th1 cells (Fig. 3 and Table I). Transcription factors vital for Th17 differentiation and cytokine production include RORγt, RORα, and, downstream from TGF-β receptor signaling, Runx1 (50, 51). WT Th17 cells expressed high levels of mRNA encoding RORα, RORγt, Smad3 and Runx1. Although the level of *Rorc* was only marginally attenuated in PARP14-null samples of developing Th17 cells, expression of *Rora*, *Smad3* and *Runx1* was substantially reduced in *Parp14* −/− Th17 cells compared to WT controls, as were mRNA levels for IL-17A and IL-22 (Fig. 3C). Thus, we conclude that PARP14 impacts components of the TGFβ response system and transcription factors that regulate the Th17 phenotype as well as Th17 differentiation and cytokine production.

$CD103^+$ dendritic cells (DCs) are major cellular sources of RA and promote both Th17 and IgA production, especially under conditions of inflammation (26, 28, 52). Based on the evidence that PARP14 acts by a B lineage-extrinsic mechanism to promote IgA responses, we measured $CD103^+$ DCs in *Parp14*−/− mice. $CD103^+$ DCs in mesenteric lymph node (MLN), intestinal epithelial compartment (IEC), and intestinal lamina propria (LP) of *Parp14* −/− mice were reduced compared to WT controls (Fig. 4A, B). A major mechanism by which $CD103^+$ DCs regulate IgA is through local enzymatic conversion of vitamin A into RA via retinol aldehyde dehydrogenase (RALDH) in these cells (28). *Aldh1a2* encodes RALDH2, the principal isoform of RALDH in IgA regulation, and *Aldh1a2* mRNA levels in the LP and IEC were lower in samples of PARP14-deficient mice compared to WT controls (Fig. 4C). Moreover, mRNA for the other two isoforms of RALDH, RALDH1 (*Aldh1a1*) and RALDH3 (*Aldh1a3*), were also lower in these *Parp14* −/− tissues (Fig. 4C). These findings indicate that the B lineage-extrinsic defect involves both the T helper subset and the major source of RA, each of which is critical for directing IgA production.

ADP ribosyltransferase activity of PARP14 is crucial for Th17 differentiation

The physiological impact of the endogenous mammalian ADP-ribosyl monotransferases is as yet completely unknown. However, pertussis and cholera exotoxins, which function by ADP-ribosylation inside mammalian target cells (53, 54), promote the Th17 response so we tested whether or not the enzymatic activity of PARP14 is critical for its function in T helper cell differentiation. To eliminate PARP14 mART activity, we generated three point mutations (PARP14^{3mut}; H1698F, Y1730N and E1810K) at the canonical PARP catalytic triad of the PARP14 enzymatic domain (Fig. 5A). ADP-ribosyltransferase activity assays with PARP14^{3mut} showed an essentially complete loss of transferase activity (Fig. 5B). To test if the impact of PARP14 on Th17 differentiation involves the mART activity, we performed retroviral reconstitutions of CD4^{+} T cells. PARP14-MC, a truncated form of PARP14 containing the middle (triple macro domains) and C-terminus (mART catalytic domain) regions, has catalytic activity and can be packaged into retrovirus virions. Activated CD4^{+} T cells lacking PARP14 were transduced with PARP14-MC, PARP14-MC^{3mut} or empty vector (MiT), cultured under Th17 conditions, and scored for differentiation efficiency compared to controls. These analyses showed that although the enzymatic activity of PARP14-MC was ~ 1/10th that of full-length PARP14 protein (Fig. 5B), PARP14-MC transduction into PARP14-deficient CD4^{+} T cells restored their efficiency of Th17 differentiation to a normal level (Fig. 5C), indicating that the defect in Th17 differentiation is reversible after T cell activation. Strikingly, however, PARP14-MC^{3mut} transduction into *Parp14* −/− CD4^{+} T cells was unable to restore normal frequencies of IL-17^{+} cells (Fig. 5C). We conclude that the ADP-ribosyltransferase activity of PARP14 plays a cell-intrinsic role in Th17 differentiation.

PARP14 promotes recall IgE and allergic responses

In vitro analyses showed that CD4^{+} IL-4^{+} T (Th2) cells differentiated less efficiently in the absence of PARP14, and the immunization studies revealed impaired recall antibody responses. These findings prompted us to investigate the impact of PARP14 on a type 2 immune response and IgE using models of primary and recall allergic lung inflammation (Fig. 6A). WT and *Parp14* −/− mice showed similar numbers of inflammatory cells in bronchoalveolar lavage (BAL) fluid after a primary response, but eosinophil numbers in the BAL of *Parp14* −/− mice were substantially reduced in their allergic memory response (Fig. 6B). Mucus secretion in lungs was also lower in *Parp14* −/− mice after a recall challenge as compared to WT mice (Fig. 6C). Consistent with the in vitro differentiation analyses, IL-4 concentrations in BAL fluids were much lower in *Parp14* −/− mice compared to WT mice after recall immunization with OVA, and IL-17 was also reduced (Fig. 6D). These results indicate that even after primary immune challenge, PARP14 promotes allergic inflammation in the memory phase, and are consistent with a role for PARP14 in CD4^{+} T cell differentiation into IL-4 and IL-17–producing cells.

PARP14-mediated IgE generation is B cell intrinsic function

T cell-derived IL-4 is essential for isotype switching to IgE, so we also tested whether PARP14 influences IgE production in the allergic lung inflammation model. Consistent with a role for PARP14 in efficient IgE generation, concentrations of IgE anti-ovalbumin were reduced in *Parp14* −/− mice after both primary and recall exposures (Fig. 7A). Indeed, the quantitative deficit in IgE production in *Parp14*−/− mice increased for the memory response (Fig. 7A and Supplemental Fig. S1H). To test if the cellular basis the defect in IgE response was the same as that we observed for IgA, we analyzed cultures of purified B cells in which activated lymphoblasts were induced to class-switch to IgE and secrete Ab. Analyses of *Parp14* −/− samples, with the B cells of *Stat6* −/− mice as controls, yielded results opposite from those obtained for IgA, in that frequencies of IgE^{+} cells were lower for PARP14-deficient B cells compared to WT controls (Fig. 7B). Consistent with the reduction in IgE^{+}

B cells, secreted IgE also was impaired in *Parp14* −/− B cells (Fig. 7C). As expected, the frequency of IgE^+ cells and secreted IgE were also impaired in the *Stat6* −/− samples (Fig. 7B, C), indicating that PARP14 contributes to IgE response in a B cell-intrinsic mechanism along with the likely effect of impaired IL-4 production by helper T cells. Collectively, these findings provide evidence that PARP14 promotes recall antibody responses using distinct cellular mechanisms in Ig class-dependent manner.

DISCUSSION

Many bacterial exotoxins execute mono ADP-ribosylation of mammalian proteins inside the target cell and serve as strong stimuli of Th17 responses in addition to acting as adjuvants (53, 54). Highly specific interactions between an exotoxin and a host adapter protein that promotes targeting of the host's intracellular substrates and the presence of ADP-ribose (ADPr)-binding domains in other microbes suggest co-evolutionary relationships that exploit normal host cell physiology (55, 56). The range of intracellular ADP-ribosyl monotransferases (mARTs) endogenous in mammalian cells (55–57) supports this possibility. However, very little is known about the physiological functions of any of the eukaryotic mARTs or of their catalytic activity. Using a loss-of-function mouse model, we show here that PARP14, a macro domain-containing mART, promotes high-affinity and recall antibody responses of several but not all isotypes, and provide evidence for distinct cellular mechanisms leading to these effects for the two heavy chain constant regions most distal from Cμ, i.e., IgA and IgE. In particular, although PARP14 exerted B cell-intrinsic function(s) that impacted the efficiency of generating IgE^+ B cells and the amount of secreted IgE, IgA regulation by PARP14 was predominantly B cell-extrinsic. The B lineage-extrinsic mechanism was consistent with a relay in which PARP14 promotes the Th17 subset in an ADP-ribosylation-dependent manner, increasing $CD103^+$ DC and RALDH in the gut and thereby enhancing the production of retinoic acid and IgA. Collectively, the findings show that PARP14 influences the class distribution, affinity repertoire, and recall capacity of antibody responses, and provide direct evidence of requirement for protein mono-ADP-ribosylation in T helper differentiation.

We observed that PARP14 mediates not only the primary IgA response but also more dramatically influences IgA production after recall challenge. This highly abundant antibody isotype differs from most Ig classes because boundary tissues direct a substantial portion of the IgA production into trans-mucosal secretion. Accordingly, luminal microbes encounter IgA prior to any tissue entry and this class of Ab appears to be a major regulator of the commensal population (58, 59). The diversity of ADP-ribosylating bacterial exotoxins (e.g., cholera, diphtheria, and pertussis toxins) that induce Th17 responses and IgA production may be a part the microbial strategy for managing the host niche (58, 59). More broadly, IgA regulation may be divided between systemic and a locally segregated enteric immunity (58). In the systemic compartment, marginal zone B (MZB) cells possess the potential to generate more IgA in vitro than conventional follicular B cells (60), and PARP14-deficient mice have a reduction (~50%) in MZB cells (35). Thus, the deficit of MZB in *Parp14* −/− mice might contribute to the impact of PARP14 deficiency on IgA. Recent studies of the enteric compartment used lineage-tracking to provide evidence that Th17-phenotype cells can morph into T_{FH}-phenotype cells and that Th17 differentiation can be essential for promoting IgA production (29). To what extent this effect is due to direct ($T_{FH}17$ – Peyer's Patch GC B cell) or indirect mechanisms or some combination thereof remains to be determined. Nonetheless, the findings strongly support the interpretation that the inefficient generation of Th17 cells from naïve *Parp14* −/− precursors is a vital part of a B cell-extrinsic mechanism for decreased IgA production. A detailed understanding remains to be elaborated, but an analogous contribution of subset-restricted cytokines to T helper effects on the Ig class distribution may be present for IFN-γ-dependent IgG isotypes. Thus,

although the magnitudes of the effects were smaller than for IgA and Th17 cells, IgG2a and IgG2b concentrations were lower in recall immunity of *Parp14* −/− mice. We also found that in addition to a CD4 T cell-intrinsic capacity of this mART to promote Th17 differentiation, enteric $CD103^+$ DCs were reduced in *Parp14* −/− mice, which may contribute to the quantitatively greater effects on IgA than other Ab classes. These DCs in turn are critical sources of retinoic acid, a key driver of B cell switching to IgA (26) and of T helper differentiation (52). The quantitative balance between mucosal and systemic rates of Ag-specific IgA production rarely is clear. All together, though, we suggest that PARP14 promotes IgA by a mechanism that includes enhancement of Th17 differentiation, $CD103^+$ DC and RALDH generation of retinoic acid, with each cell type important for the efficient production of IgA.

We also found that Ag-specific IgE levels, Th2 and Th17 cytokines as well as airway eosinophils were reduced in a recall model of allergic lung inflammation. Recent work has provided parallel evidence that PARP14 impacts a primary immune response leading to allergic lung inflammation and IgE anti-ovalbumin (61). Intriguingly, our data revealed no reduction in pulmonary inflammation after the primary exposure, yet upon recall challenge major markers of Th2 inflammation (eosinophil recruitment; IL-4) were halved. Since the same model allergen was used, this disparity of results most likely was due to differences in priming between the two studies. Notwithstanding this point, our results indicate that PARP14 can influence the intensity of a recall response under conditions where the primary episode of inflammation was unaffected in *Parp14* −/− mice. A striking feature of IgE physiology is that, in contrast to other Ab classes, Cε-switched B cells are impersistent in germinal center reactions, associated with a limited capacity to form IgE^+ memory B cells and long-lived ASC (14, 46). Thus, recall IgE responses start from a lower baseline and exhibit major contributions of secondary switching to Cε from Cγ1 (14). The penetrance of an effect of PARP14 only on recall IgE in our experiments suggests the speculative possibility that, in vivo, the expression of this ART may better facilitate sterile IgH Cε transcription in the setting of secondary switching or memory B cells than primary or naïve counterparts. Alternatively, although preliminary in vitro analyses did not reveal increased *Prdm1* mRNA or Blimp1 protein in *Parp14* −/− B cells, these characteristics may be due to prematurely dominant expression of Blimp-1, a master regulator of plasma cells suppressor of B cell identity (45).. In part, the defect of Th2 differentiation efficiency in vitro suggests that part of the weaker memory response in the PARP14-deficient mice is attributable to weaker Th2 differentiation in vivo. However, another possibility is raised by work indicating that in anti-helminthic immunity, the strength of memory Th2 inflammation is sustained at least in part by a subset of B lymphocytes (62). In this regard, it is notable that the absence of PARP14 impeded effects of c-Myc on B cell physiology (36), and that recent findings highlight that this proto-oncogene is highly expressed in GC B cells and essential for supporting a sustained GC reaction (38, 39). Thus, because aspects of B cell physiology are altered in the absence of PARP14, an intriguing possibility is that the decrease in IgE memory manifested in recall allergic inflammation is due at least in part to impairment of *Parp14* −/− B cells.

A key finding of this study is that the capacity to reverse impaired Th17 differentiation in *Parp14* −/− T cells required the protein's catalytic function, as there has previously not been any evidence of such a requirement for intracellular mammalian mARTs in normal cell physiology. The mammalian family of intracellular proteins with a domain similar to the catalytic PARP moiety has 17 members, of which PARP1 was first identified and acts as a processive polymerase (57). Several PARP proteins lack enzymatic activity, others have not been assessed, and the rest are either polymerases ('true PARPs') or likely mono-ARTs. A major emphasis of research in this area has been on critical roles of poly-(ADP-ribosyl)ation in DNA damage responses and cancer, an exciting feature of which is the emergence of

PARP inhibitors with evidence of efficacy in clinical trials (63). Moreover, although polymerase-independent as well as polymerase-dependent functions of PARP1 have been reported (64, 65), the absence of the protein alters several aspects of inflammatory responses (66). In parallel, animal studies have used similar nicotinamide or NAD^+ analogues to show beneficial effects on models of inflammation such as inflammatory arthritis (67), Helicobacter-induced gastric pre-neoplasia in IL-10-deficient mice (68), and allergic airway inflammation (61, 66). However, there are no specific inhibitors for PARP14 and virtually none for PARP1. Existing PARP inhibitors are NAD^+ analogues that bind to a portion of each catalytic domain that is structurally similar among PARP family members. Both empiric testing of inhibition by commercially available compounds, and a recent biophysical analysis that evaluated the small molecule inhibitors for their ability to bind various PARP family members, showed that essentially all PARP inhibitors interacted similarly with the various PARPs including PARP14 (63). For instance, PJ-34 completely blocks PARP14 as well as PARP1 and other PARPs activity (35). Inasmuch as PARP14 can mediate processes on which PARP1 has no identifiable impact (35), the findings here raise important questions about inhibitor studies in vivo as well as analyses of conventional PARPs capable of executing branching polymerization. Thus, critical assessments of which PARP family member(s) are affected by such inhibitors will be vital. Since the Th17 response is active in Helicobacter infection (69) and analyses of T helper differentiation of *Parp1* −/− and *Parp2* −/− lymphocytes failed to yield a defect observed for PJ-34 inhibition, it may be that PARP14 is the active target of PJ-34 therapy in the setting of gastric inflammation and pre-neoplasia (68). Moreover, although PJ-34 has been reported to inhibit Th2 differentiation in vitro, we could observe this inhibitory effect only at concentrations causing high levels of T cell death and, as noted, cell-free assays indicate that PARP1 and PARP14 exhibit comparable inhibitory concentration curves with PJ-34 (unpublished observations). Conversely transduction of the catalytically inactive PARP14-MC into *Parp14* −/− CD4 T cells developing in Th2 conditions reversed the Th2 differentiation defect (unpublished observations). All together, the results suggest that PJ-34 affects Th2 cell differentiation predominantly by a PARP14-independent mechanism, and this protein's ART activity may be dispensable for Th2 differentiation yet a cell-intrinsic signal promoting Th17 function.

Supplementary Material

Refer to Web version on PubMed Central for supplementary material.

Acknowledgments

We thank S. Han and B. Saville (Dept. of Biostatistics, Vanderbilt University) for statistical consultation and expertise.

Supported by National Institute of Health grant R01 AI077528 and HL106812 to M.B.

Abbreviations used

PARP	Poly-(ADP-Ribose) Polymerase
ART	(ADP-ribosyl) transferase
NP	4-Hydroxy-3-nitrophenylacetyl
NIP	4-Hydroxy-3-iodo-5-nitrophenylacetyl
KLH	Keyhole Limpet Hemocyanin
MPV	metapneumovirus

ASC	Ab-secreting cells
RA	retinoic acid
RALDH	retinol aldehyde dehydrogenase
BAL	bronchoalveolar lavage
PAS	Periodic acid-Schiff

References

1. Pulendran B, Ahmed R. Immunological mechanisms of vaccination. Nat Immunol. 2011; 12:509–517. [PubMed: 21739679]
2. McHeyzer-Williams M, Okitsu S, Wang N, McHeyzer-Williams L. Molecular programming of B cell memory. Nat Rev Immunol. 2012; 12:24–34. [PubMed: 22158414]
3. Nutt SL, Tarlinton DM. Germinal center B and follicular helper T cells: siblings, cousins or just good friends? Nat Immunol. 2011; 12:472–477. [PubMed: 21739669]
4. Wabl M, Steinberg C. Affinity maturation and class switching. Curr Opin Immunol. 1996; 8:89–92. [PubMed: 8729451]
5. Dullaers M, De Bruyne R, Ramadani F, Gould HJ, Gevaert P, Lambrecht BN. The who, where, and when of IgE in allergic airway disease. J Allergy Clin Immunol. 2012; 129:635–645. [PubMed: 22168998]
6. Ishizaka T, Sian CM, Ishizaka K. Complement fixation by aggregated IgE through alternate pathway. J Immunol. 1972; 108:848–851. [PubMed: 4551855]
7. Russell MW, Mansa B. Complement-fixing properties of human IgA antibodies. Alternative pathway complement activation by plastic-bound, but not specific antigen-bound, IgA. Scand J Immunol. 1989; 30:175–183. [PubMed: 2762767]
8. Macpherson AJ, Geuking MB, McCoy KD. Homeland security: IgA immunity at the frontiers of the body. Trends Immunol. 2012; 33:160–167. [PubMed: 22410243]
9. Takai T. Fc receptors and their role in immune regulation and autoimmunity. J Clin Immunol. 2005; 25:1–18. [PubMed: 15742153]
10. Goodnow CC, Vinuesa CG, Randall KL, Mackay F, Brink R. Control systems and decision making for antibody production. Nat Immunol. 2010; 11:681–688. [PubMed: 20644574]
11. Zotos D, Tarlinton DM. Determining germinal centre B cell fate. Trends Immunol. 2012; 33:281–288. [PubMed: 22595532]
12. Shlomchik MJ, Weisel F. Germinal center selection and the development of memory B and plasma cells. Immunol Rev. 2012; 247:52–63. [PubMed: 22500831]
13. Geha RS, Jabara HH, Brodeur SR. The regulation of immunoglobulin E class-switch recombination. Nat Rev Immunol. 2003; 3:721–732. [PubMed: 12949496]
14. Xiong H, Dolpady J, Wabl M, Curotto de Lafaille MA, Lafaille JJ. Sequential class switching is required for the generation of high affinity IgE antibodies. J Exp Med. 2012; 209:353–364. [PubMed: 22249450]
15. Finkelman FD, Holmes J, Urban JF Jr, Paul WE, Katona IM. T help requirements for the generation of an in vivo IgE response: a late acting form of T cell help other than IL-4 is required for IgE but not for IgG1 production. J Immunol. 1989; 142:403–408. [PubMed: 2521345]
16. Glatman Zaretsky A, Taylor JJ, King IL, Marshall FA, Mohrs M, Pearce EJ. T follicular helper cells differentiate from Th2 cells in response to helminth antigens. J Exp Med. 2009; 206:991–999. [PubMed: 19380637]
17. King IL, Mohrs M. IL-4-producing CD4+ T cells in reactive lymph nodes during helminth infection are T follicular helper cells. J Exp Med. 2009; 206:1001–1007. [PubMed: 19380638]
18. Hou J, Schindler U, Henzel WJ, Ho TC, Brasseur M, McKnight SL. An interleukin-4-induced transcription factor: IL-4 Stat. Science. 1994; 265:1701–1706. [PubMed: 8085155]

19. Kaplan MH, Schindler U, Smiley ST, Grusby MJ. Stat6 is required for mediating responses to IL-4 and for development of Th2 cells. Immunity. 1996; 4:313–319. [PubMed: 8624821]
20. Shimoda K, van Deursen J, Sangster MY, Sarawar SR, Carson RT, Tripp RA, Chu C, Quelle FW, Nosaka T, Vignali DA, Doherty PC, Grosveld G, Paul WE, Ihle JN. Lack of IL-4-induced Th2 response and IgE class switching in mice with disrupted Stat6 gene. Nature. 1996; 380:630–633. [PubMed: 8602264]
21. Linehan LA, Warren WD, Thompson PA, Grusby MJ, Berton MT. STAT6 is required for IL-4-induced germline Ig gene transcription and switch recombination. J Immunol. 1998; 161:302–310. [PubMed: 9647237]
22. Messner B, Stutz AM, Albrecht B, Peiritsch S, Woisetschlager M. Cooperation of binding sites for STAT6 and NF kappa B/rel in the IL-4-induced up-regulation of the human IgE germline promoter. J Immunol. 1997; 159:3330–3337. [PubMed: 9317131]
23. Cerutti A. The regulation of IgA class switching. Nat Rev Immunol. 2008; 8:421–434. [PubMed: 18483500]
24. Watanabe K, Sugai M, Nambu Y, Osato M, Hayashi T, Kawaguchi M, Komori T, Ito Y, Shimizu A. Requirement for Runx proteins in IgA class switching acting downstream of TGF-beta 1 and retinoic acid signaling. J Immunol. 2010; 184:2785–2792. [PubMed: 20142360]
25. Fagarasan S. Evolution, development, mechanism and function of IgA in the gut. Curr Opin Immunol. 2008; 20:170–177. [PubMed: 18456485]
26. Mora JR, Iwata M, Eksteen B, Song SY, Junt T, Senman B, Otipoby KL, Yokota A, Takeuchi H, Ricciardi-Castagnoli P, Rajewsky K, Adams DH, von Andrian UH. Generation of gut-homing IgA-secreting B cells by intestinal dendritic cells. Science. 2006; 314:1157–1160. [PubMed: 17110582]
27. Dubin PJ, Kolls JK. Th17 cytokines and mucosal immunity. Immunol Rev. 2008; 226:160–171. [PubMed: 19161423]
28. Hall JA, Grainger JR, Spencer SP, Belkaid Y. The role of retinoic acid in tolerance and immunity. Immunity. 2011; 35:13–22. [PubMed: 21777796]
29. Hirota K, Turner JE, Villa M, Duarte JH, Demengeot J, Steinmetz OM, Stockinger B. Plasticity of TH17 cells in Peyer's patches is responsible for the induction of T cell-dependent IgA responses. Nat Immunol. 2013; 14:372–379. [PubMed: 23475182]
30. Shockett P, Stavnezer J. Effect of cytokines on switching to IgA and alpha germline transcripts in the B lymphoma I.29 mu. Transforming growth factor-beta activates transcription of the unrearranged C alpha gene. J Immunol. 1991; 147:4374–4383. [PubMed: 1753105]
31. Murray PD, McKenzie DT, Swain SL, Kagnoff MF. Interleukin 5 and interleukin 4 produced by Peyer's patch T cells selectively enhance immunoglobulin A expression. J Immunol. 1987; 139:2669–2674. [PubMed: 3498768]
32. Rasmussen R, Takatsu K, Harada N, Takahashi T, Bottomly K. T cell-dependent hapten-specific and polyclonal B cell responses require release of interleukin 5. J Immunol. 1988; 140:705–712. [PubMed: 2448371]
33. Stevens TL, Bossie A, Sanders VM, Fernandez-Botran R, Coffman RL, Mosmann TR, Vitetta ES. Regulation of antibody isotype secretion by subsets of antigen-specific helper T cells. Nature. 1988; 334:255–258. [PubMed: 2456466]
34. Goenka S, Boothby M. Selective potentiation of Stat-dependent gene expression by collaborator of Stat6 (CoaSt6), a transcriptional cofactor. Proc Natl Acad Sci U S A. 2006; 103:4210–4215. [PubMed: 16537510]
35. Cho SH, Goenka S, Henttinen T, Gudapati P, Reinikainen A, Eischen CM, Lahesmaa R, Boothby M. PARP-14, a member of the B aggressive lymphoma family, transduces survival signals in primary B cells. Blood. 2009; 113:2416–2425. [PubMed: 19147789]
36. Cho SH, Ahn AK, Bhargava P, Lee CH, Eischen CM, McGuinness O, Boothby M. Glycolytic rate and lymphomagenesis depend on PARP14, an ADP ribosyltransferase of the B aggressive lymphoma (BAL) family. Proc Natl Acad Sci U S A. 2011; 108:15972–15977. [PubMed: 21911376]

37. Barbarulo A, Iansante V, Chaidos A, Naresh K, Rahemtulla A, Franzoso G, Karadimitris A, Haskard DO, Papa S, Bubici C. Poly(ADP-ribose) polymerase family member 14 (PARP14) is a novel effector of the JNK2-dependent pro-survival signal in multiple myeloma. Oncogene. 2012
38. Calado DP, Sasaki Y, Godinho SA, Pellerin A, Kochert K, Sleckman BP, de Alboran IM, Janz M, Rodig S, Rajewsky K. The cell-cycle regulator c-Myc is essential for the formation and maintenance of germinal centers. Nat Immunol. 2012; 13:1092–1100. [PubMed: 23001146]
39. Dominguez-Sola D, Victora GD, Ying CY, Phan RT, Saito M, Nussenzweig MC, Dalla-Favera R. The proto-oncogene MYC is required for selection in the germinal center and cyclic reentry. Nat Immunol. 2012; 13:1083–1091. [PubMed: 23001145]
40. Lee K, Gudapati P, Dragovic S, Spencer C, Joyce S, Killeen N, Magnuson MA, Boothby M. Mammalian target of rapamycin protein complex 2 regulates differentiation of Th1 and Th2 cell subsets via distinct signaling pathways. Immunity. 2010; 32:743–753. [PubMed: 20620941]
41. Aronica MA, Mora AL, Mitchell DB, Finn PW, Johnson JE, Sheller JR, Boothby MR. Preferential role for NF-kappa B/Rel signaling in the type 1 but not type 2 T cell-dependent immune response in vivo. J Immunol. 1999; 163:5116–5124. [PubMed: 10528218]
42. Lutzker S, Rothman P, Pollock R, Coffman R, Alt FW. Mitogen- and IL-4-regulated expression of germ-line Ig gamma 2b transcripts: evidence for directed heavy chain class switching. Cell. 1988; 53:177–184. [PubMed: 2834063]
43. Erickson JJ, Gilchuk P, Hastings AK, Tollefson SJ, Johnson M, Downing MB, Boyd KL, Johnson JE, Kim AS, Joyce S, Williams JV. Viral acute lower respiratory infections impair CD8+ T cells through PD-1. J Clin Invest. 2012; 122:2967–2982. [PubMed: 22797302]
44. Cox RG, Livesay SB, Johnson M, Ohi MD, Williams JV. The human metapneumovirus fusion protein mediates entry via an interaction with RGD-binding integrins. J Virol. 2012; 86:12148–12160. [PubMed: 22933271]
45. Yang Z, Sullivan BM, Allen CD. Fluorescent in vivo detection reveals that IgE(+) B cells are restrained by an intrinsic cell fate predisposition. Immunity. 2012; 36:857–872. [PubMed: 22406270]
46. Talay O, Yan D, Brightbill HD, Straney EE, Zhou M, Ladi E, Lee WP, Egen JG, Austin CD, Xu M, Wu LC. IgE(+) memory B cells and plasma cells generated through a germinal-center pathway. Nat Immunol. 2012; 13:396–404. [PubMed: 22366892]
47. Sheridan BS, Lefrancois L. Isolation of mouse lymphocytes from small intestine tissues. Curr Protoc Immunol. 2012; Chapter 3(Unit 3):19. [PubMed: 23129154]
48. Reth M, Hammerling GJ, Rajewsky K. Analysis of the repertoire of anti-NP antibodies in C57BL/6 mice by cell fusion. I. Characterization of antibody families in the primary and hyperimmune response. Eur J Immunol. 1978; 8:393–400. [PubMed: 97089]
49. Kaminski DA, Stavnezer J. Stimuli that enhance IgA class switching increase histone 3 acetylation at S alpha, but poorly stimulate sequential switching from IgG2b. Eur J Immunol. 2007; 37:240–251. [PubMed: 17163453]
50. Collins A, Littman DR, Taniuchi I. RUNX proteins in transcription factor networks that regulate T-cell lineage choice. Nat Rev Immunol. 2009; 9:106–115. [PubMed: 19165227]
51. Yang XO, Pappu BP, Nurieva R, Akimzhanov A, Kang HS, Chung Y, Ma L, Shah B, Panopoulos AD, Schluns KS, Watowich SS, Tian Q, Jetten AM, Dong C. T helper 17 lineage differentiation is programmed by orphan nuclear receptors ROR alpha and ROR gamma. Immunity. 2008; 28:29–39. [PubMed: 18164222]
52. Hall JA, Cannons JL, Grainger JR, Dos Santos LM, Hand TW, Naik S, Wohlfert EA, Chou DB, Oldenhove G, Robinson M, Grigg ME, Kastenmayer R, Schwartzberg PL, Belkaid Y. Essential role for retinoic acid in the promotion of CD4(+) T cell effector responses via retinoic acid receptor alpha. Immunity. 2011; 34:435–447. [PubMed: 21419664]
53. Andreasen C, Powell DA, Carbonetti NH. Pertussis toxin stimulates IL-17 production in response to Bordetella pertussis infection in mice. PLoS One. 2009; 4:e7079. [PubMed: 19759900]
54. Datta SK, Sabet M, Nguyen KP, Valdez PA, Gonzalez-Navajas JM, Islam S, Mihajlov I, Fierer J, Insel PA, Webster NJ, Guiney DG, Raz E. Mucosal adjuvant activity of cholera toxin requires Th17 cells and protects against inhalation anthrax. Proc Natl Acad Sci U S A. 2010; 107:10638–10643. [PubMed: 20479237]

55. O'Neal CJ, Jobling MG, Holmes RK, Hol WG. Structural basis for the activation of cholera toxin by human ARF6-GTP. Science. 2005; 309:1093–1096. [PubMed: 16099990]
56. Corda D, Di Girolamo M. Functional aspects of protein mono-ADP-ribosylation. EMBO J. 2003; 22:1953–1958. [PubMed: 12727863]
57. Hassa PO, Haenni SS, Elser M, Hottiger MO. Nuclear ADP-ribosylation reactions in mammalian cells: where are we today and where are we going? Microbiol Mol Biol Rev. 2006; 70:789–829. [PubMed: 16959969]
58. Hooper LV, Littman DR, Macpherson AJ. Interactions between the microbiota and the immune system. Science. 2012; 336:1268–1273. [PubMed: 22674334]
59. Kamada N, Nunez G. Role of the gut microbiota in the development and function of lymphoid cells. J Immunol. 190:1389–1395. [PubMed: 23378581]
60. Kaminski DA, Stavnezer J. Enhanced IgA class switching in marginal zone and B1 B cells relative to follicular/B2 B cells. J Immunol. 2006; 177:6025–6029. [PubMed: 17056527]
61. Mehrotra P, Hollenbeck A, Riley JP, Li F, Patel RJ, Akhtar N, Goenka S. Poly (ADP-ribose) polymerase 14 and its enzyme activity regulates T(H)2 differentiation and allergic airway disease. J Allergy Clin Immunol. 2013; 131:521–531. e521–512. [PubMed: 22841009]
62. Wojciechowski W, Harris DP, Sprague F, Mousseau B, Makris M, Kusser K, Honjo T, Mohrs K, Mohrs M, Randall T, Lund FE. Cytokine-producing effector B cells regulate type 2 immunity to H. polygyrus. Immunity. 2009; 30:421–433. [PubMed: 19249230]
63. Wahlberg E, Karlberg T, Kouznetsova E, Markova N, Macchiarulo A, Thorsell AG, Pol E, Frostell A, Ekblad T, Oncu D, Kull B, Robertson GM, Pellicciari R, Schuler H, Weigelt J. Family-wide chemical profiling and structural analysis of PARP and tankyrase inhibitors. Nat Biotechnol. 2012; 30:283–288. [PubMed: 22343925]
64. Kim MY, Mauro S, Gevry N, Lis JT, Kraus WL. NAD+-dependent modulation of chromatin structure and transcription by nucleosome binding properties of PARP-1. Cell. 2004; 119:803–814. [PubMed: 15607977]
65. Pavri R, Lewis B, Kim TK, Dilworth FJ, Erdjument-Bromage H, Tempst P, de Murcia G, Evans R, Chambon P, Reinberg D. PARP-1 determines specificity in a retinoid signaling pathway via direct modulation of mediator. Mol Cell. 2005; 18:83–96. [PubMed: 15808511]
66. Luo X, Kraus WL. On PAR with PARP: cellular stress signaling through poly(ADP-ribose) and PARP-1. Genes Dev. 26:417–432. [PubMed: 22391446]
67. Gonzalez-Rey E, Martinez-Romero R, O'Valle F, Aguilar-Quesada R, Conde C, Delgado M, Oliver FJ. Therapeutic effect of a poly(ADP-ribose) polymerase-1 inhibitor on experimental arthritis by downregulating inflammation and Th1 response. PLoS One. 2007; 2:e1071. [PubMed: 17971849]
68. Toller IM, Altmeyer M, Kohler E, Hottiger MO, Muller A. Inhibition of ADP ribosylation prevents and cures helicobacter-induced gastric preneoplasia. Cancer Res. 2010; 70:5912–5922. [PubMed: 20634404]
69. Algood HM, Allen SS, Washington MK, Peek RM Jr, Miller GG, Cover TL. Regulation of gastric B cell recruitment is dependent on IL-17 receptor A signaling in a model of chronic bacterial infection. J Immunol. 2009; 183:5837–5846. [PubMed: 19812196]

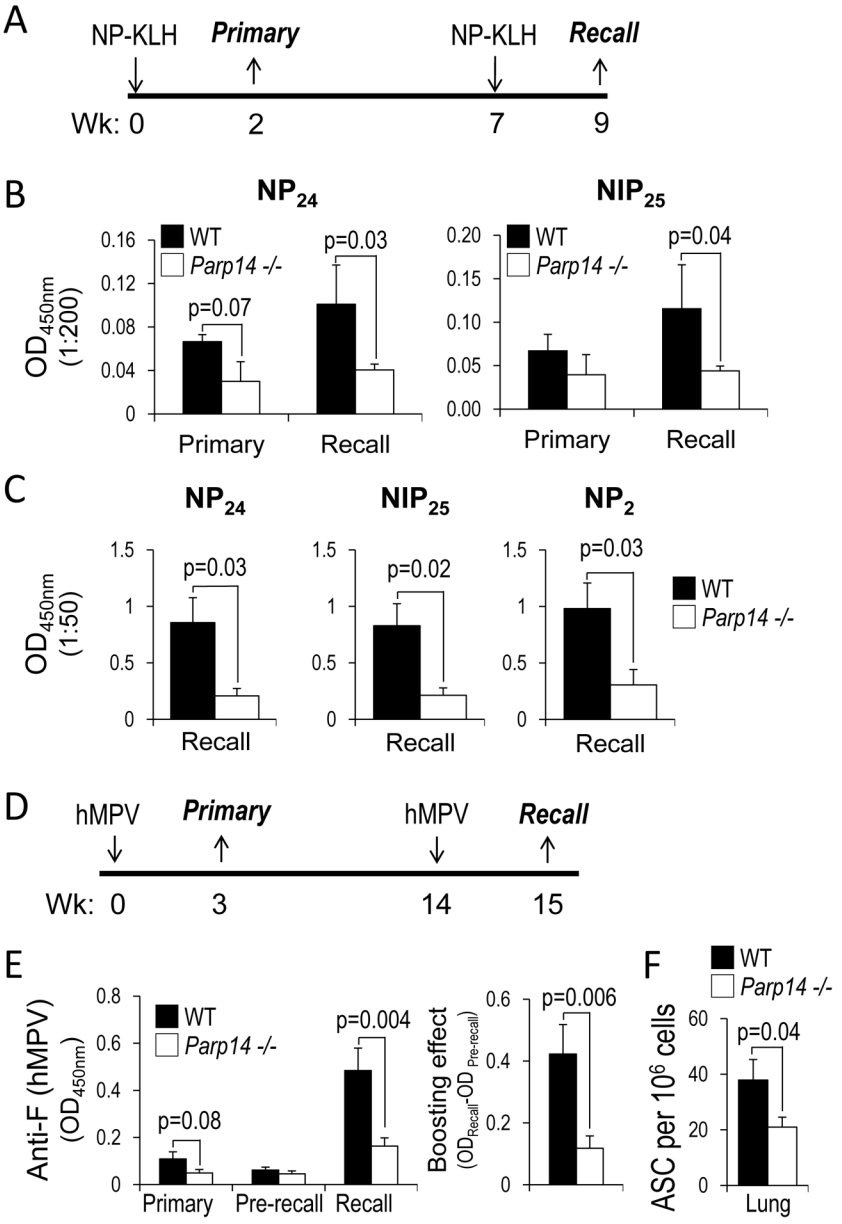

Figure 1.

PARP14 promotes recall IgA production. (A) Schedule of immunizations for testing anti-hapten Ab responses. After collecting pre-immune samples, sera from WT and *Parp14 −/−* mice (6 wks; n=14 each) immunized with NP_{25}-KLH in alum and subjected to recall challenge at 7 weeks post-immunization were sampled as indicated. (B, C) Levels of IgA specific for Ag (NP_{24}-BSA)-, of related specificity (NIP_{25}-BSA)-, or high-affinity (NP_2-PSA) were measured using capture ELISA as described in *Materials and Methods*. Bar graphs show mean (± SEM) OD_{450nm} from measurements at 1:200 (B) and 1:50 (C) dilutions of these sera in measurements validated by determinations of relative concentrations by titration (Supplemental Figure 1G). (D-F) PARP14 mediates anti-viral IgA production after infection. (D) Schedule of human metapneumovirus (hMPV) infection and re-challenge. WT and *Parp14 −/−* mice were infected with hMPV, maintained for 12 wk after virus clearance (7–10 d), and then re-challenged. Sera for measurements of anti-viral

Ab were collected as indicated. (E) hMPV-specific IgA levels in primary and recall immune sera (1:400 dilutions) were determined using purified recombinant hMPV F (surface fusion) protein. (F) hMPV F-specific IgA-secreting cells in lung were analyzed by ELISPOT assay as described in *Materials and Methods*.

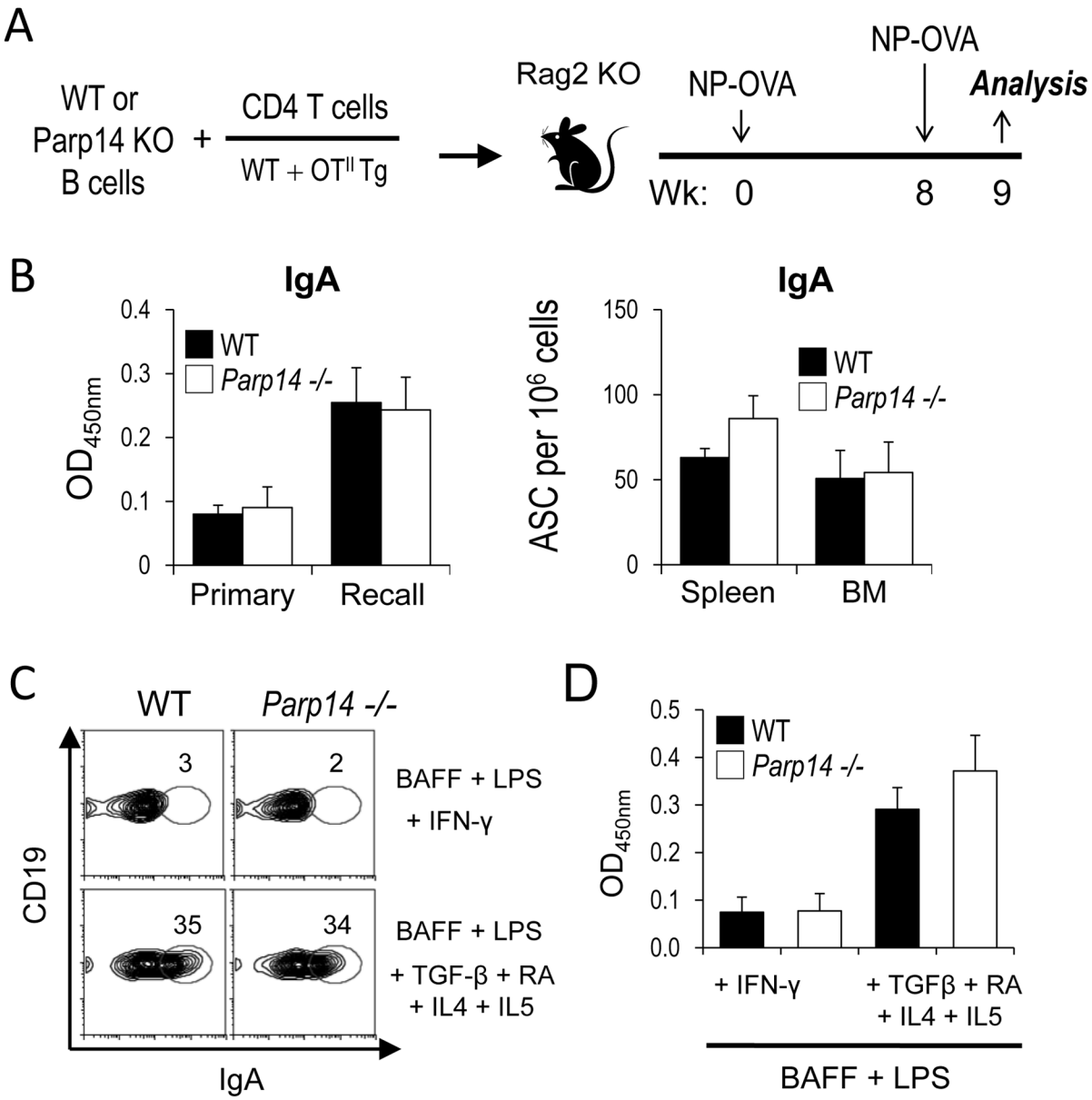

Figure 2.

B cell-extrinsic role of PARP14 in IgA production. (A) Schema of the adoptive transfer model. B cells from WT or *Parp14 −/−* mice were mixed with WT CD4$^+$ T cells (a 4:1 mixture of CD4$^+$ T cells of B6 and OT-II mice), transferred into syngeneic *Rag2 −/−* recipients, immunized with NP-OVA at the indicated times, and harvested 1 wk after recall immunization. (B) Shown are mean (±SEM) OD_{450nm} of Ag-specific IgA levels in primary and recall immune sera (1:200 dilutions) (left panel) as well as frequencies of Ag-specific IgA-secreting cells in bone marrow and spleen (right panel) after recall challenge of adoptive transfer mice (two biologically independent replicate experiments comprising 8 mice of each genotype). (C, D) After determination of conditions for maximal IgA production, B cells from WT and *Parp14 −/−* mice were activated with LPS and cultured in the presence of BAFF with IFN-γ (to estimate pre-committed B cells) or TGFβ, RA, IL-4, and IL-5 for 5 days. Frequencies of surface IgA$^+$ cells among B220$^+$-gated cells (C) and

secreted IgA in cultures (D) were measured. Bar graphs show mean (±SEM) values from three independent experiments.

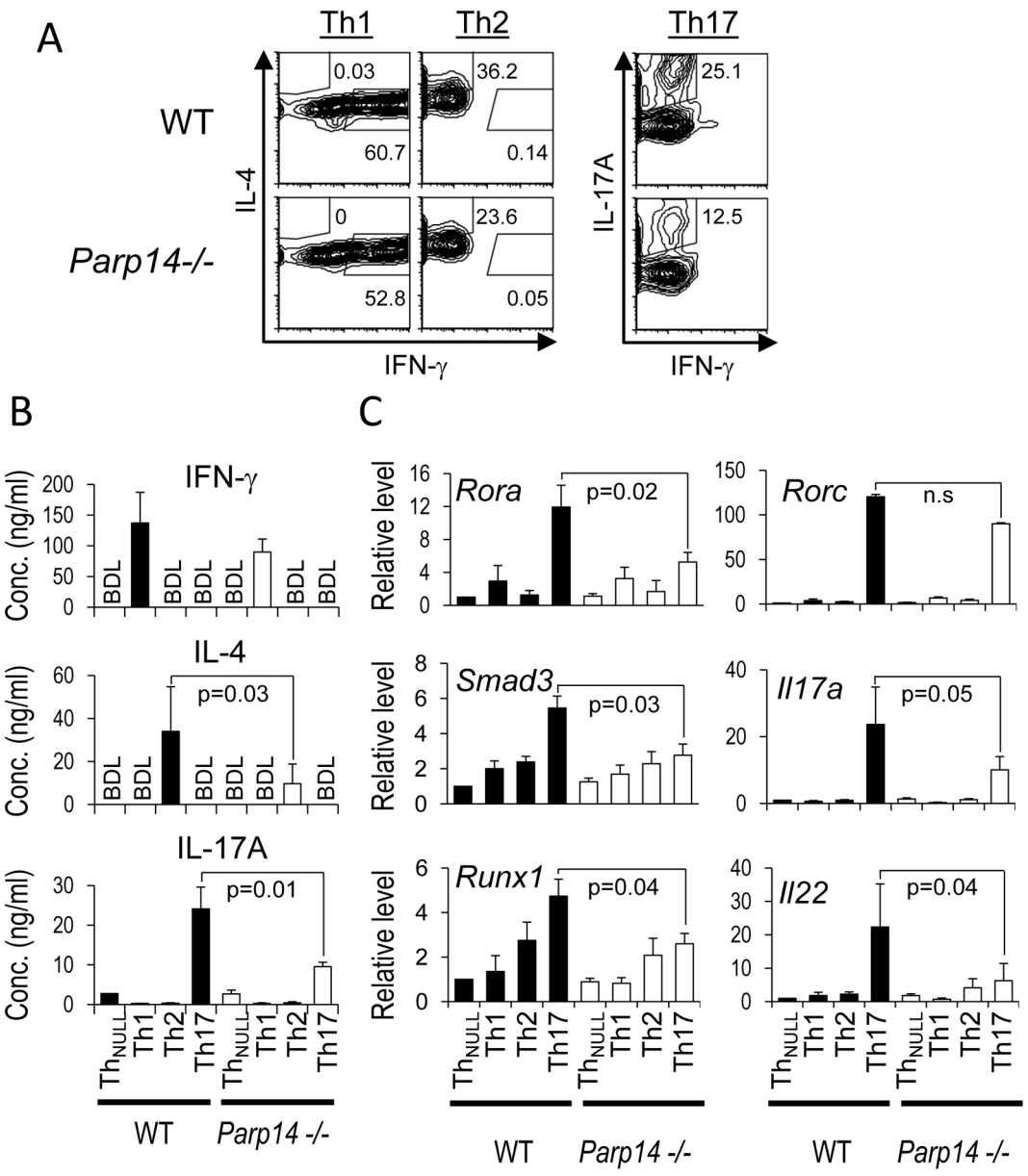

Figure 3.

PARP14 and T helper cell differentiation. (A, B) Naïve CD4$^+$ T cells from WT and *Parp14 −/−* mice were cultured under Th1, Th2 and Th17 differentiating conditions for 5 d after activation with αCD3 and αCD28. Equal numbers of viable cells were then re-stimulated (αCD3 and αCD28), and the indicated cytokines were detected by intracellular staining (A) and as secreted proteins in culture supernatants (B). Bar graphs show mean (± SEM) cytokine concentrations from replicates in four independent experiments. (C) Naïve CD4$^+$ T cells from WT and *Parp14 −/−* mice were activated with αCD3 plus αCD28, cultured under null (Th_{NULL}), Th1, Th2 and Th17 conditions for 5 d. Transcript levels were measured by quantitative real-time RT-PCR normalized to HPRT signal in the sample and then to the level in WT Th_{NULL} cells (set as relative level of 1) of the particular experiment. Bar graphs show mean (±SEM) relative expression measured in samples from four independent culture experiments.

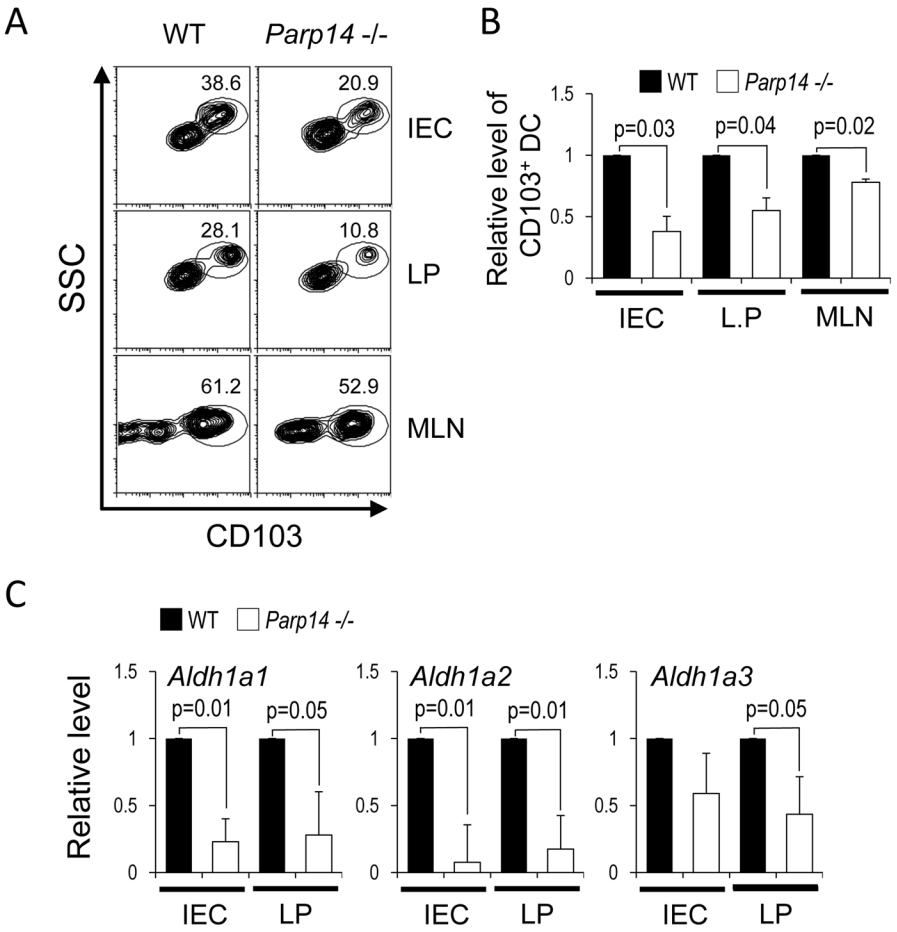

Figure 4.

Reduced levels of retinaldehyde dehydrogenase (RALDH) and CD103^{+}DC in guts of *Parp14* $-/-$ mice. (A, B) Frequencies of CD103^{+} DC. Single cell suspensions of intra-epithelial (IEC), lamina propria (LP) and mesenteric LN (MLN) were analyzed by flow cytometry as described in the *Methods*. Shown are representative FACS profiles in the CD11c^{+} CD11b^{-} gate (A) and a graph (B) of the mean (±SEM) relative level of cells in three independent replicate analyses. (C) Levels of mRNA encoded by the *Aldh1a1*, -2 and -3 genes (RALDH1-3) were measured by quantitative real-time RT-PCR after preparation of total RNA from IEC and LP suspensions. Bar graphs show mean (± SEM) expression (relative to HPRT in the sample) measured in four (IEC) or six (LP) independent replicate preparations.

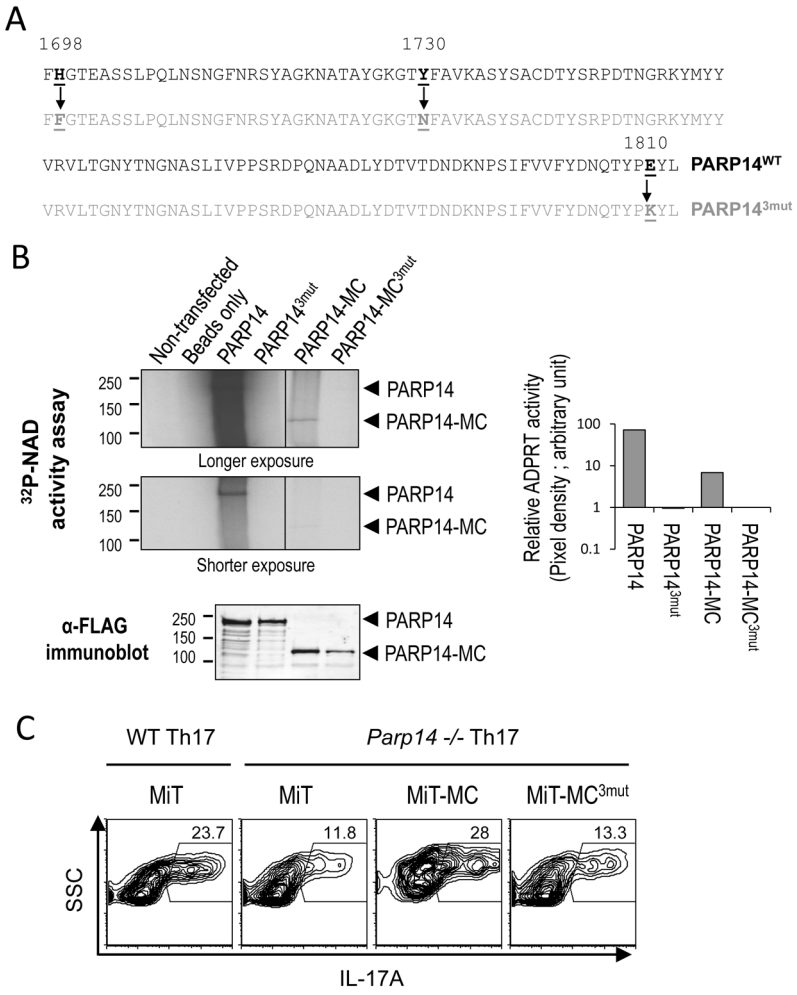

Figure 5.

ART-dependent reversion of Th17 differentiation of PARP14-deficient T cells. (A) Amino acid sequence spanning the presumptive catalytic triad of PARP14 catalytic C domain and the point-mutated residues in PARP14^{3mut} (34). (B) Proteins from cells transfected with FLAG epitope-tagged PARP-14, PARP-14^{3mut}, PARP-14-MC or PARP-14-MC^{3mut} were precipitated with anti-FLAG. One aliquot of bead-bound immune complexes was assayed for transfer of ^{32}P-labeled ADP-ribose from NAD^{+} onto proteins, while the other part was used for immunoblotting to measure the relative amounts of purified PARP14 in each sample. Shown are autoradiographs (upper left panel) and immunoblots to determine protein levels (lower left panel) after resolution by SDS-PAGE. Arrowheads mark the expected positions for full-length PARP14 and PARP14-MC. (Right panel) Phosphor-Imager quantitations (in arbitrary units of pixel density) of the radioactive signal for each band normalized to the protein level determined from the immunoblots. (C) PARP14 and its ADP-ribosyltransferase activity are required for optimal Th17 differentiation. CD4^{+} T cells were activated under non-differentiating conditions, transduced to express PARP14-MC or –MC^{3mut}, cultured (5 d) under Th17 cell differentiating condition, re-stimulated and analyzed by flow cytometry. Shown are representative FACS profiles of IL-17A in the transduced (Thy1.1^{+}) CD4^{+} gate.

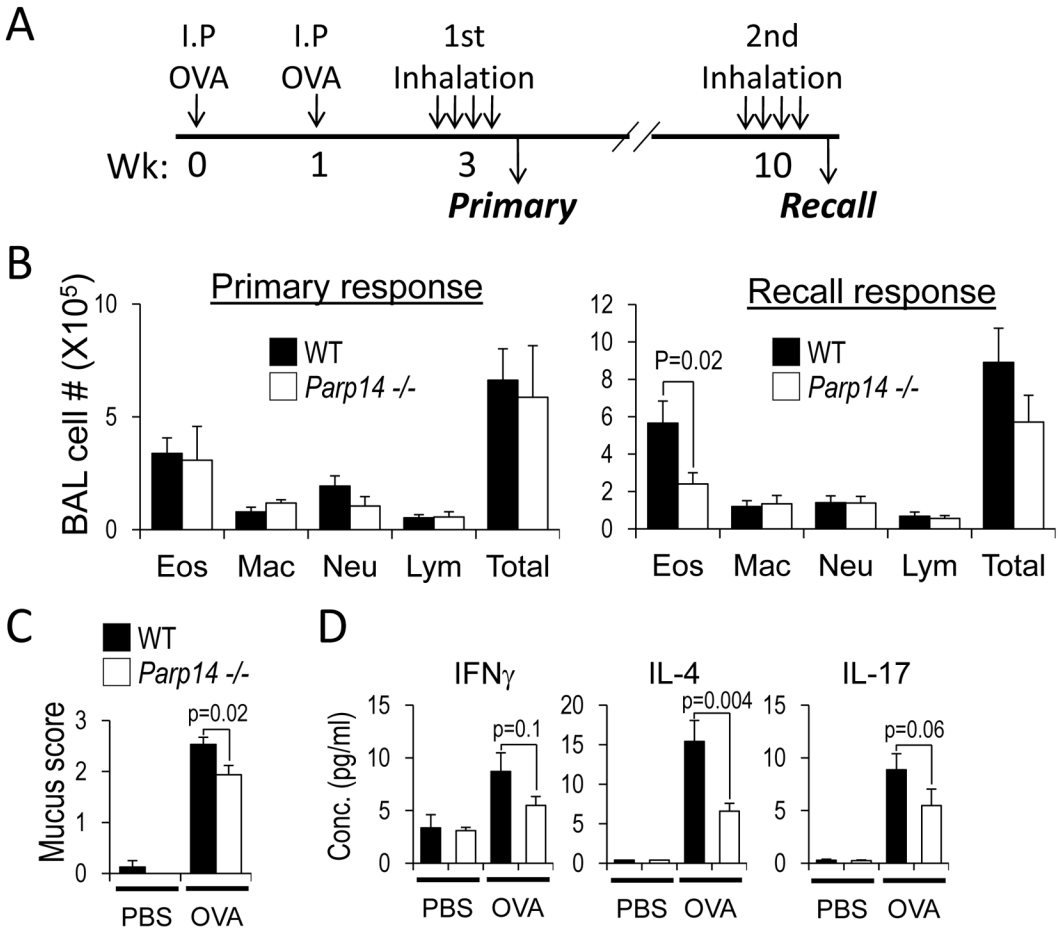

Figure 6.

Attenuated recall responses and allergic lung inflammation in the absence of PARP14. (A) For primary responses, WT and *Parp14 −/−* mice were sensitized with ovalbumin in alum followed by intranasal (i.n.) instillation of Ag on each of 4 consecutive days. Recall IgE and allergic inflammation were elicited by four daily i.n. instillations of Ag 7 wk after primary allergic experience. (B) Inflammatory cells in the BAL fluid (left, primary responses; right, recall responses). (C) Airway mucin analyzed in PAS-stained paraffin-embedded lung sections. Bar graphs show mean (±SEM) of relative mucin levels measured in three independent recall experiments. (D) Levels of T helper cytokines in the BAL fluid after recall challenge with OVA or saline (PBS). Bar graphs show mean (± SEM) cytokine concentrations obtained in three independent experiments (totaling 12 mice of each genotype).

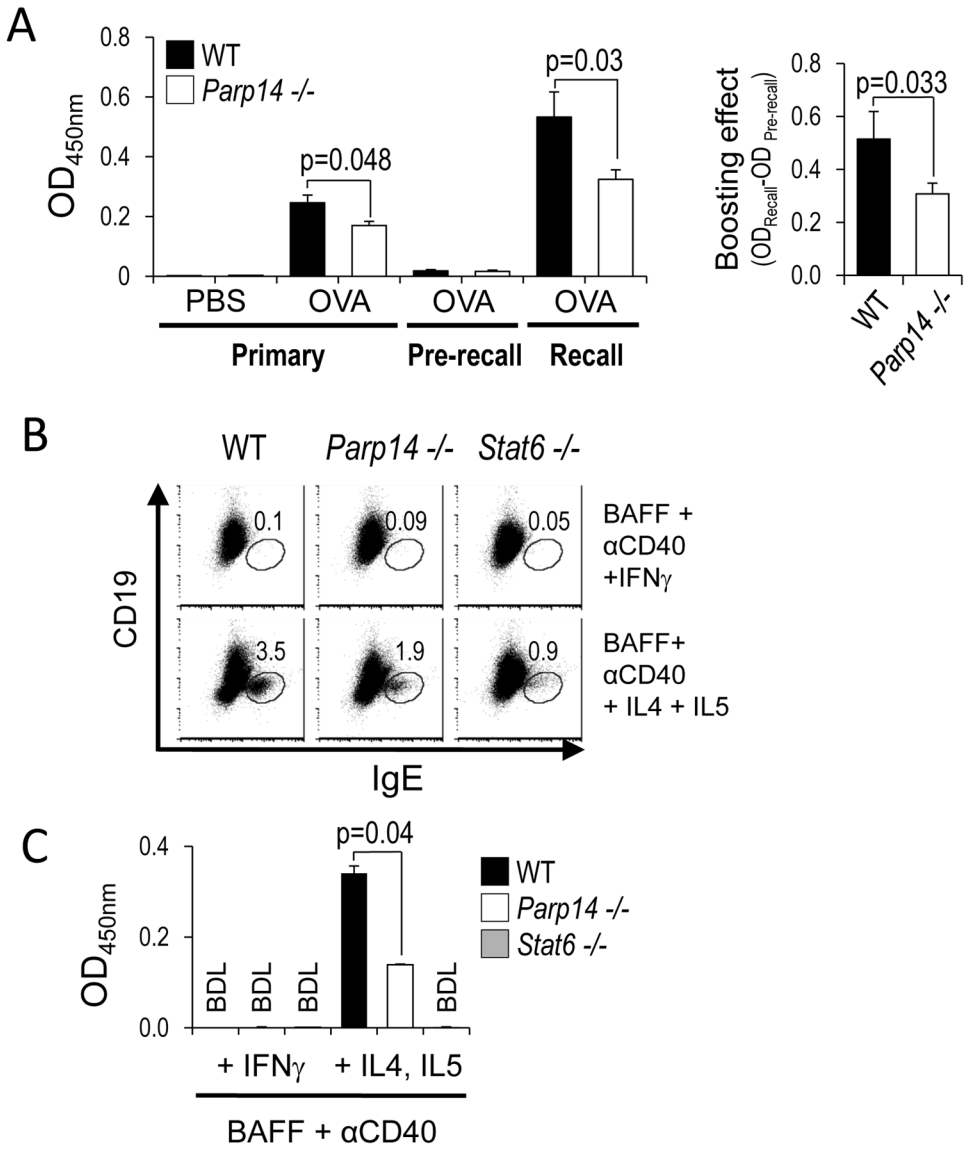

Figure 7.

Impaired Ag-specific IgE responses in *Parp14* −/− mice. (A) Serum levels of OVA-specific IgE from the OVA-induced recall allergic lung inflammation mice (Fig. 6A) were measured by capture ELISA. Bar graphs show mean (± SEM) OD_{450nm} from measurements at 1:200 dilutions of the sera from all three independent experiments (totaling 12 mice of each genotype), in measurements validated by determinations of relative concentrations by titration (Supplemental Figure 1H). (B, C) Naïve B cells from WT, *Parp14* −/−, and *Stat6* −/− mice were activated with αCD40 and cultured 5 d in the indicated cytokines. Frequencies of intracellular IgE^+ cells in $B220^+$-gated cells (B) and secreted IgE in culture medium (C) were measured. Shown are (B) a result from one representative experiment and (C) bar graphs with mean (± SEM) values obtained in three independent experiments.

Table I

Effect of PARP14 on T helper cytokine level

Genotype/cell culture	Th1 (IFN-γ)	Th2 (IL-4)	Th17 (IL-17A)
WT	68.9 ± 7.3 [a]	35.7 ± 4.5	23.9 ± 1.7
Parp14 −/−	60.2 ± 8.2 [b]	26.6 ± 5.5 [b]	14.1 ± 0.9 [b]

[a] Mean ± SEM % cytokine+ cells measured in the CD4+ viable lymphocyte gates in three independent biological replicate experiments measuring efficiency of T helper subset differentiation as described in the Methods.

[b] $p<0.05$ for the null hypothesis that no difference between WT and *Parp14 −/−* samples, as determined by two-tailed Student's t-testing.